

STATISTICAL PROPERTIES OF GRB AFTERGLOW PARAMETERS AS EVIDENCE OF COSMOLOGICAL EVOLUTION OF THEIR HOST GALAXIES

GREGORY BESKIN^{a, d,*}, GOR OGANESEYAN^b, GIUSEPPE GRECO^c,
SERGEY KARPOV^{a, d}

^a Special Astrophysical Observatory of the Russian Academy of Sciences, Nizhnij Arkhyz, Karachevo-Cherkessia, Russia

^b Southern Federal University, 5 Sorge st., Rostov-on-Don, Russia

^c Astronomical Department of Bologna University, Bologna, Italy

^d Kazan Federal University, Kazan, Russia

* corresponding author: beskin@sao.ru

ABSTRACT. The results of a study of 43 peaked R-band light curves of optical counterparts of gamma-ray bursts with known redshifts are presented. The parameters of optical transients were calculated in the comoving frame, and then a search for pair correlations between them was conducted. A statistical analysis showed a strong correlation between the peak luminosity and the redshift both for pure afterglows and for events with residual gamma activity, which cannot be explained as an effect of observational selection. This suggests a cosmological evolution of the parameters of the local interstellar medium around the sources of the gamma-ray burst. In the models of forward and reverse shock waves, a relation between the density of the interstellar medium and the redshift was built for gamma-ray burst afterglows, leading to a power-law dependence of the star-formation rate at regions around GRBs on redshift with a slope of about 6.

KEYWORDS: gamma-ray bursts, optical afterglows, statistical study.

1. INTRODUCTION

Until now, about 250 gamma-ray bursts (GRBs) with measured redshifts are known [1, 2]. Optical R-band light curves with distinct peaks have been obtained for 43 cases only. These are the most interesting objects for detailed analysis, as the presence of a peak allows us to identify the moment of shock wave deceleration in the interstellar medium, which reflects the parameters of the interstellar medium. Among 43 such events, 11 are prompt optical peaks (P), coincident with gamma-ray activity (three events that may not be unambiguously classified as P were signed as P?), 22 are pure afterglows (A), and 10 more carry the signatures of an underlying gamma-activity (A(U)). The latter group are events with continuing gamma-ray activity during the afterglow onset. Detailed results of the investigation of correlations of different pairs of GRBs parameters in these subsamples are given in [3]. In this paper, we present an analysis of connections between several optical characteristics of GRBs in the source rest frame and their redshifts.

2. OBSERVATIONAL DATA

R-band optical data, as well as other parameters of GRBs, were taken from publications dedicated to specific bursts: GRB 990123 [4], GRB 050820A [5, 6], GRB 050904 [7, 8], GRB 060418 [9], GRB 060526 [10], GRB 060605 [11], GRB 060607A [12], GRB 060729 [13],

GRB 060904B [14], GRB 061007 [13], GRB 061121 [15], GRB 070411 [16–22], GRB 070419A [23], GRB 071010A [24], GRB 071010B [25], GRB 071025 [26], GRB 071031 [27], GRB 080129 [28], GRB 080210 [29–33], GRB 080310 [34], GRB 080319B [35], GRB 080603A [36], GRB 080710 [37], GRB 080810 [38], GRB 080928 [39], GRB 081007 [40], GRB 081008 [41], GRB 081203A [42], GRB 090313 [43], GRB 090530 [44, 45], GRB 090726 [46], GRB 090812 [47, 48], GRB 091029 [49], GRB 100901A [50], GRB 100906A [50], GRB 110205A [51], GRB 110213A [52]. The initial observational parameters were as follows: the spectroscopic redshift z , the peak optical flux F_{opt} , the integral optical flux S_{opt} defined by numerical integration of light curve $F_{\text{opt}}(t)$, the time of the peak onset relative to the GRB trigger t_{peak} , the width of the optical peak t_{width} as the duration of a light curve interval with flux exceeding $0.9F_{\text{opt}}$, the exponents α_r and α_d of the growth and decay of the optical light curve $F_{\text{opt}} \propto t^{\alpha_r}$ and $F_{\text{opt}} \propto t^{-\alpha_d}$, the GRB peak gamma-ray flux F_{iso} , the GRB integral gamma-ray flux S_{iso} , the GRB duration t_{90} and the photon index of the spectrum in the gamma-ray range α . Parameters of GRBs are taken from [53].

Considering galactic extinction and host galaxy brightness, and using the k-correction $k(z)$ for the average index of optical spectrum $\beta = 0.75$ [54], $F_\nu \propto \nu^{-\beta}$, in the standard cosmological model with $\Omega_M = 0.3$, $\Omega_\Lambda = 0.7$, $H_0 = 70 \text{ km s}^{-1} \text{ Mpc}^{-1}$, we

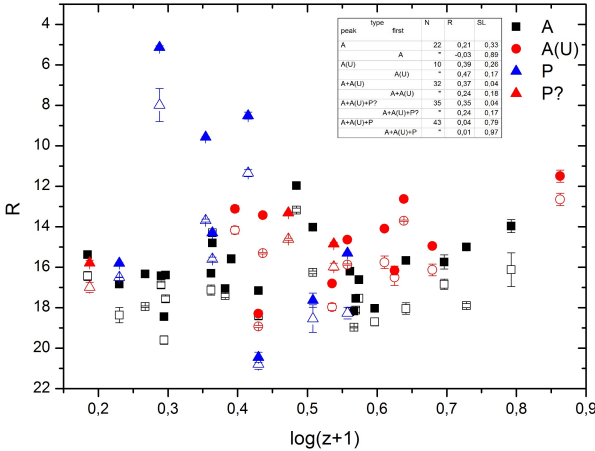


FIGURE 1. Peak and initial optical magnitudes vs. redshift: coefficients of correlations, SL.

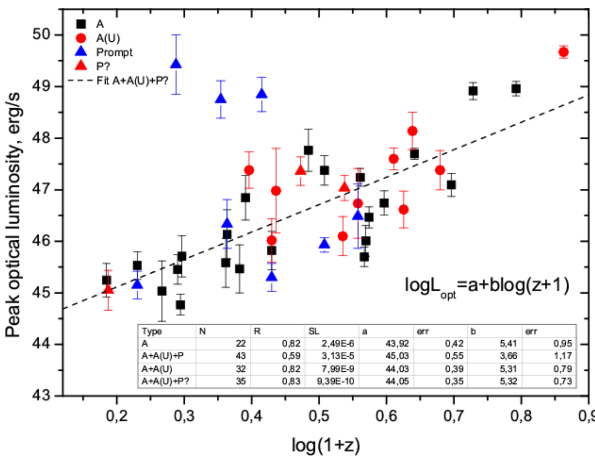


FIGURE 2. Peak optical luminosity vs. redshift: coefficients of correlations, SL, parameters of linear regression.

obtained the following parameters in the rest frame of the source: the maximum optical luminosity L_{opt} as $L_{\text{opt}} = 4\pi D^2 k(z) F_{\text{opt}}$ (where D is the luminosity distance), the isotropic equivalent of optical energy E_{opt} as a numerical integral of $L_R(t)$, the time parameters T_{peak} , T_{width} as $T_{\text{peak}} = \frac{t_{\text{peak}}}{(1+z)}$, $T_{\text{width}} = \frac{t_{\text{width}}}{(1+z)}$, and, in the gamma-ray range, L_{iso} , E_{iso} from [53], $T_{90} = \frac{t_{90}}{(1+z)}$. For the bursts whose host galaxy extinction A_R is not available, the mean value of A_R was utilized instead, using the A_V data collected in the golden sample presented by [55]. These data were divided into five redshift ranges and for each interval the corresponding mean value of A_V was obtained. Using these estimates along with the dependence of absorption on wavelength in SMC [56], the A_R for each burst was computed. The formulae for conversion from the observed frame to the rest frame are taken from [3]. Table 2 presents all pair correlations with unweighted Pearson correlation coefficients $R > 0.5$ and significance levels SL better than 0.01, and the coefficients of the corresponding linear regressions.

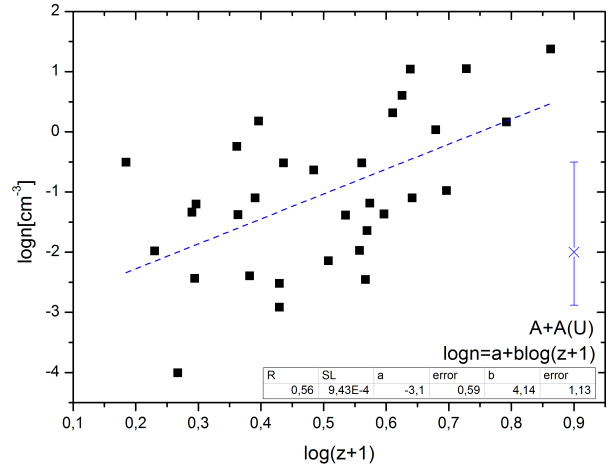


FIGURE 3. ISM density vs. redshift by model recalculations.

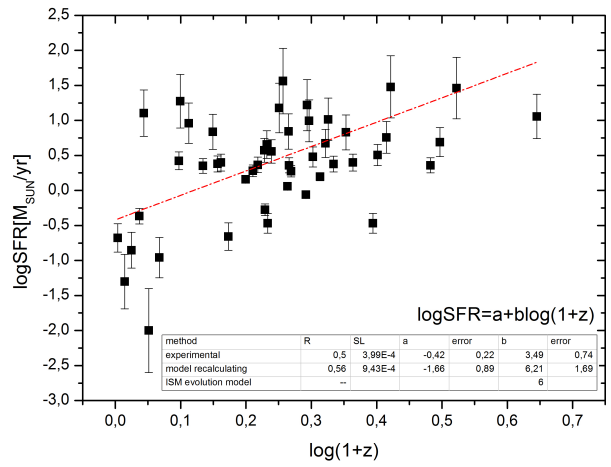


FIGURE 4. SFR vs. redshift correlation.

3. RESULTS AND DISCUSSIONS

To prove that the correlation between peak optical luminosity and the redshift is not caused by selection effects, we plot (Figure 1) the R-band apparent magnitudes of all bursts at the initial moment of optical detection (empty symbols) and at the moment of maximum (filled symbols) versus the redshift. Note that the signatures of selection effects should be searched for in the set of initial brightness estimates in the first place. Let us discuss whether they are present in our data.

- (1.) Obviously, if the rest frame luminosities of sources do not increase with the redshift (i.e., the luminosity is the same on all z), then the apparent brightness (flux measured by the observer) will decrease at least quadratically with $(1+z)$. At the same time, (Figure 1) demonstrates a significant increase in brightness at $z > 3$, both for the moments of detection and for the peaks.
- (2.) For both large ($z > 3$) and small ($z < 1$) redshifts the objects are brighter than 18 mag, significantly brighter than the minimum value of 19–19.5 mag achieved by several objects at $1 < z < 3$. Therefore,

neither small nor large z display any signs of bias due to crossing the detection limit line — both bright and faint sources are being detected on all redshifts.

(3.) Finally, referring to the $L_{\text{opt}} : z$ dependence (Figure 2), we checked the correlation coefficients and linear regression parameters for the $A + A(U) + P?$ subset in different redshift ranges. They are summarized in Table 1.

It is easy to see that even with the exclusion of objects with $z < 1$ or with $z > 4$, or both, the luminosity still increases with the redshift with good significance. Obviously, the correlation coefficient decreases a bit with decreasing redshift range, but the regression parameters are nearly the same within the errors, and the power-law slope of the dependence is roughly 4–5. Therefore, our analysis demonstrates that observational selection effects which may cause the dependence of optical luminosity in peaks of light curves on the redshift, are most probably absent in our data.

To check the validity of the correlations found between the peak luminosity of the afterglow and the redshift, we simulated the ensemble of 100000 events with luminosities normally distributed in logarithms with mean 46 and dispersion 2, as estimated from the luminosity function used in [57]. The absorption (Galactic and host) has a uniform distribution in the range $0 < A_R < 3$, and the index of the optical spectrum is uniformly distributed between $0.2 < \beta < 1.2$. The limits for β and A_R (recalculated by A_V) are taken from observations [55]. Modifying the A_R and β parameters of the distribution function does not change the results of the simulation. From this sample, we repeatedly (2000 times) randomly selected realizations of 40 bursts brighter than 23 magnitude in the R-band, and computed for each one the Pearson's correlation coefficient r between the optical luminosity and the redshift. We considered two ensembles — with luminosity independent from redshift, and with the ensemble scaling as $L_{\text{opt}} \sim (1+z)^4$. In the former case, the number of realizations with $r > 0.6$ was 4, and in the latter case, the number of realizations with $r < 0.8$ was 1. In other words, the probability of first type error (accidental detection of the effect in the absence thereof) for the strong positive correlation of luminosity and redshift is close to 0.002, and for the second type error it is 0.0005. So there is reason to believe that the rapid growth of the optical luminosity of the afterglow with redshift is a real physical dependence, and it is not an effect of a small sample or observational selection.

We may consider the detected $L_{\text{opt}} : (z+1)$ correlation (Figure 2) as a real manifestation of the cosmological evolution of the optical luminosity of gamma-ray burst afterglows.

There is no $L_{\text{opt}} : (z+1)$ correlation for prompt optical sources, in contrast to the strong correlation

seen for afterglows. Prompt optical events (P) are presumably produced as a result of collisions of internal shells in GRB sources, while the afterglows are formed as the shock wave enters the interstellar medium. The peak in an afterglow optical light curve arises from deceleration of the blast wave. This process depends on a local interstellar medium and the initial conditions of the shock wave [58]. The simplest assumption is dependence of the local interstellar medium density on the redshift, which results in the observed $L_{\text{opt}} : (z+1)$ dependence.

In the afterglow model with the front shock wave, the peak flux is a function of density, as we may assume that the frequency of the optical emission lies between the characteristic frequency of the radiation and the cooling frequency. Indeed, according to [59], if the frequency of the afterglow spectral peak ν_i is lower than the cooling frequency ν_c , then the optical spectrum index is $p = \frac{(b-1)}{2}$, where p is a spectral index of emitting electrons, $2 < p < 3$ [60], and $0.5 < \beta < 1$. If, on the other hand, the peak is in the $\nu > \nu_c$ region, then $\beta = p/2$ and $1 < \beta < 1.5$. At the same time, observations of optical spectra give $\beta < 1$ [61] with an average value of $\beta = 0.75$, and therefore our assumption is correct. Then, according to [62], $F \sim En^{\frac{(p-1)}{2}} \Gamma_0^{4\beta}$, where E is the total mechanical energy, n is the volume density of the surrounding gas, Γ_0 is the initial Lorentz factor of the ejecta, and β is the index of the optical spectrum. Using a rough estimate of $\Gamma_0 = 200$ with dispersion of 100 [63, 64], the peak luminosity L_{opt} , $E_{\text{iso}} = \eta E$ ($\eta = 0.2$ from [65]), and the deceleration radius $R_{\text{dec}} \sim t_{\text{dec}} \Gamma_0^2$ [66], where $T_{\text{peak}} = t_{\text{dec}}$, $L_{\text{opt}} \sim R_{\text{dec}}^2 F$, $n \sim \frac{L_{\text{opt}}}{T_{\text{peak}} k^2 E_{\text{iso}} r_0^8}$ we obtain power-law dependence with a slope of 4.14 ± 1.13 (Figure 3). With this dependence in hand, we may build a similar dependence for the star formation rate (SFR) in the vicinity of the GRBs, using the Kennicutt-Schmidt law from [67]: the star formation rate depends on the volume density of the interstellar medium as $\text{SFR} \sim n^{1.5}$. Finally, we acquired $\text{SFR} \sim (1+z)^{6.21 \pm 1.69}$.

Using the values of SFR taken from the GRB-Hosts [68] database, we compared them to this relation. This is shown in Figure 4, which also shows the model value of this dependence based on the ratios for the interstellar medium density from [69] and the volume law of Kennicutt-Schmidt.

The obtained $\text{SFR} : (z+1)$ dependence is consistent with the model dependence from [69], but it differs from the experimental correlation for the host galaxies from the GRB-Hosts database (the slope of correlation $\text{SFR} : (z+1)$ is 3.49 ± 0.74) and from [70] (the slope is 3.38 ± 0.69). Also, our result differs from these theoretical model from [71], where the slope is 2.71. In our opinion, this fact reflects the difference of the characteristics (the rate in the first place) of star formation in compact regions surrounding gamma-ray bursts about 0.1 pc in size, and of these processes in the galaxy as a whole.

z	N	R	SL	a	Error	b	Error
All	35	0.83	$9.39 \cdot 10^{-10}$	44.05	0.35	5.32	0.73
$z < 4$	32	0.73	$1.73 \cdot 10^{-6}$	44.29	0.37	4.71	0.80
$z < 1$	31	0.78	$1.91 \cdot 10^{-7}$	44.12	0.5	5.2	0.97
$1 < z < 4$	28	0.60	$7.31 \cdot 10^{-4}$	44.55	0.55	4.22	1.11

TABLE 1. Characteristics of the dependence of optical luminosity on redshift for A + A(U) + P? subset in different redshift ranges. Columns are the redshift range, number of sources in it, correlation coefficient, its significance level, and the linear regression parameters (a, b) with corresponding errors.

Correlation	Type	N	R	SL	a	Error	b	Error
$E_{\text{iso}} : L_{\text{iso}}$	P	10	0.89	$4.97 \cdot 10^{-4}$	1.58	5.60	0.99	0.11
	A	22	0.89	$4.10 \cdot 10^{-8}$	5.04	6.78	0.93	0.13
	A + A(U) + P	41	0.88	$6.39 \cdot 10^{-14}$	5.09	4.31	0.92	0.08
	A + A(U)	31	0.87	$1.30 \cdot 10^{-10}$	7.34	5.67	0.88	0.11
	A + A(U) + P?	34	0.88	$4.64 \cdot 10^{-12}$	8.20	4.91	0.86	0.09
$E_{\text{opt}} : L_{\text{opt}}$	P	11	0.88	$3.25 \cdot 10^{-4}$	11.62	7.14	0.80	0.15
	A	22	0.88	$1.70 \cdot 10^{-8}$	12.91	4.57	0.80	0.10
	A(U)	10	0.76	$1.08 \cdot 10^{-2}$	28.63	0.43	0.46	0.14
	A + A(U) + P	43	0.77	$1.80 \cdot 10^{-9}$	17.45	4.89	0.69	0.09
	A + A(U)	32	0.85	$7.76 \cdot 10^{-10}$	17.76	3.65	0.69	0.08
	P-3	8	0.87	$3.32 \cdot 10^{-3}$	9.87	8.85	0.83	0.19
	A + A(U) + P?	35	0.83	$6.40 \cdot 10^{-10}$	17.26	3.82	0.70	0.08
$E_{\text{opt}} : E_{\text{iso}}$	P	11	0.76	$6.92 \cdot 10^{-3}$	-20.74	19.69	1.32	0.37
	A	22	0.73	$1.25 \cdot 10^{-4}$	-4.20	11.40	1.03	0.22
	A + A(U) + P	43	0.61	$1.45 \cdot 10^{-5}$	-1.28	10.31	0.20	0.36
	A + A(U)	32	0.74	$1.65 \cdot 10^{-6}$	-3.03	8.91	1.01	0.17
	P-3	8	0.86	$6.09 \cdot 10^{-3}$	-40.95	21.49	1.70	0.41
	A + A(U) + P?	35	0.7	$2.59 \cdot 10^{-6}$	-1.8	9.16	0.98	0.17
$L_{\text{opt}} : z + 1$	A	22	0.82	$2.49 \cdot 10^{-6}$	43.92	0.42	5.41	0.95
	A + A(U) + P	43	0.59	$3.13 \cdot 10^{-5}$	45.03	0.55	3.66	1.17
	A + A(U)	32	0.82	$7.99 \cdot 10^{-9}$	44.03	0.39	5.31	0.79
	A + A(U) + P?	35	0.83	$9.39 \cdot 10^{-10}$	44.05	0.35	5.32	0.73
$E_{\text{opt}} : L_{\text{iso}}$	A	22	0.66	$7.40 \cdot 10^{-4}$	2.09	12.02	0.93	0.23
	A(U)	9	0.83	$5.31 \cdot 10^{-3}$	-24.50	18.63	1.44	0.36
	A + A(U) + P	41	0.62	$1.80 \cdot 10^{-5}$	2.88	9.55	0.91	0.18
	A + A(U)	31	0.70	$1.08 \cdot 10^{-5}$	-0.39	9.49	0.97	0.18
	A + A(U) + P?	34	0.67	$1.28 \cdot 10^{-5}$	2.80	9.22	0.91	0.18
$E_{\text{opt}} : T_{\text{width}}$	P	11	-0.78	$4.41 \cdot 10^{-3}$	53.49	1.22	-3.94	1.04
	P-3	8	-0.81	$1.44 \cdot 10^{-2}$	54.28	1.61	-4.45	1.32
$L_{\text{opt}} : E_{\text{iso}}$	A	22	0.79	$1.21 \cdot 10^{-5}$	-32.3	13.2	1.50	0.25
	A + A(U) + P	43	0.75	$6.21 \cdot 10^{-9}$	-30.16	11.95	1.46	0.23
	A + A(U)	32	0.76	$4.70 \cdot 10^{-7}$	-44.11	11.60	1.73	0.22
	A + A(U) + P?	35	0.76	$1.15 \cdot 10^{-7}$	-41.69	11.14	1.69	0.21
$L_{\text{opt}} : L_{\text{iso}}$	A	22	0.77	$2.55 \cdot 10^{-5}$	-27.03	11.95	1.43	0.23
	A + A(U) + P	41	0.76	$8.25 \cdot 10^{-9}$	-29.88	10.01	1.49	0.19
	A + A(U)	31	0.78	$2.91 \cdot 10^{-7}$	-37.96	9.85	1.65	0.19
	A + A(U) + P?	34	0.76	$1.67 \cdot 10^{-7}$	-32.90	9.65	1.55	0.19

(continued on the next page)

(cont.)

Correlation	Type	<i>N</i>	<i>R</i>	<i>SL</i>	<i>a</i>	Error	<i>b</i>	Error
$E_{\text{iso}} : z + 1$	A	22	0.82	$3.69 \cdot 10^{-6}$	50.84	0.28	3.49	0.58
	A + A(U) + P	43	0.60	$2.07 \cdot 10^{-5}$	51.73	0.31	2.17	0.61
	A + A(U)	32	0.73	$1.82 \cdot 10^{-6}$	51.09	0.28	2.98	0.52
	A + A(U) + P?	35	0.75	$2.70 \cdot 10^{-7}$	51.09	0.26	3.01	0.49
$L_{\text{opt}} : T_{\text{peak}}$	P	11	-0.77	$5.16 \cdot 10^{-3}$	52.73	2.03	-3.86	1.24
$T_{\text{peak}} : T_{\text{width}}$	A	22	0.65	$9.20 \cdot 10^{-4}$	1.24	0.24	0.51	0.13
	A + A(U) + P	43	0.76	$2.57 \cdot 10^{-9}$	1.00	0.13	0.59	0.08
	A + A(U)	32	0.72	$4.07 \cdot 10^{-6}$	1.22	0.16	0.50	0.09
	A + A(U) + P?	35	0.74	$3.00 \cdot 10^{-7}$	1.16	0.14	0.53	0.08
$E_{\text{opt}} : z + 1$	A	22	0.67	$5.50 \cdot 10^{-4}$	47.90	0.51	4.26	1.03
	A + A(U)	32	0.67	$2.66 \cdot 10^{-5}$	48.09	0.41	3.89	0.78
	A + A(U) + P	43	0.57	$6.43 \cdot 10^{-5}$	47.81	0.46	4.13	0.93
	A + A(U) + P?	35	0.69	$4.56 \cdot 10^{-6}$	47.92	0.39	4.11	0.75
$L_{\text{iso}} : z + 1$	A	22	0.73	$1.21 \cdot 10^{-4}$	50.28	0.36	2.86	0.77
	A + A(U) + P	41	0.59	$5.10 \cdot 10^{-5}$	50.82	0.32	2.11	0.66
	A + A(U)	31	0.72	$5.23 \cdot 10^{-6}$	50.39	0.29	2.66	0.56
	A + A(U) + P?	34	0.74	$6.70 \cdot 10^{-7}$	50.30	0.28	2.82	0.55
* $E_{\text{opt}} : \alpha_{\text{decay}}$	A	22	-0.59	$4.23 \cdot 10^{-3}$	48.89	0.36	-1.01	0.32
* $L_{\text{opt}} : \alpha_{\text{decay}}$	A	22	-0.55	$8.64 \cdot 10^{-3}$	46.11	0.46	-0.88	0.35

TABLE 2. Pair correlations for different classes of GRB optical counterparts with correlation coefficients greater than 0.5 and significances better than 1%. The four columns represent the linear regression ($a + bx$) coefficients, derived through the unweighted least squares fit. The stars mark the log-linear correlations, in contrast to the log-log correlations used otherwise.

ACKNOWLEDGEMENTS

This work was supported by RFBR No. 12-02-00743. S.K. has also been supported by a grant from the non-profit Dynasty foundation. G.B. thanks Landau Network-Centro Volta and the Cariplo Foundation for a fellowship and the Brera Observatory for hospitality.

REFERENCES

- [1] N. Gehrels, S. Razzaque. Gamma-ray bursts in the swift-Fermi era. *Frontiers of Physics* **8**:661–678, 2013. [arXiv:1301.0840](https://arxiv.org/abs/1301.0840) doi:10.1007/s11467-013-0282-3.
- [2] D. M. Coward, E. J. Howell, M. Branchesi, et al. The Swift gamma-ray burst redshift distribution: selection biases and optical brightness evolution at high z ? *MNRAS* **432**:2141–2149, 2013. [arXiv:1210.2488](https://arxiv.org/abs/1210.2488) doi:10.1093/mnras/stt537.
- [3] G. Beskin, G. Greco, G. Oganesyan, S. Karpov. On Some Statistical Properties of GRBs with Measured Redshifts Having Peaks in Optical Light Curves. *Acta Polytechnica* **53**(3):030000, 2013.
- [4] T. J. Galama, M. S. Briggs, R. A. M. J. Wijers, et al. Spectral Energy Distributions and Light Curves of GRB 990123 and its Afterglow. *ArXiv Astrophysics e-prints* 1999. [arXiv:astro-ph/9903021](https://arxiv.org/abs/astro-ph/9903021).
- [5] W. T. Vestrand, J. A. Wren, P. R. Wozniak, et al. Energy input and response from prompt and early optical afterglow emission in γ -ray bursts. *Nature* **442**:172–175, 2006. [arXiv:astro-ph/0605472](https://arxiv.org/abs/astro-ph/0605472) doi:10.1038/nature04913.
- [6] S. B. Cenko, M. Kasliwal, F. A. Harrison, et al. Multiwavelength Observations of GRB 050820A: An Exceptionally Energetic Event Followed from Start to Finish. *ApJ* **652**:490–506, 2006. [arXiv:astro-ph/0608183](https://arxiv.org/abs/astro-ph/0608183) doi:10.1086/508149.
- [7] D. A. Kann, N. Masetti, S. Klose. The Prompt Optical/Near-Infrared Flare of GRB 050904: The Most Luminous Transient Ever Detected. *AJ* **133**:1187–1192, 2007. [arXiv:astro-ph/0606567](https://arxiv.org/abs/astro-ph/0606567) doi:10.1086/511066.
- [8] G. Tagliaferri, L. A. Antonelli, G. Chincarini, et al. GRB 050904 at redshift 6.3: observations of the oldest cosmic explosion after the Big Bang. *A&A* **443**:L1–L5, 2005. [arXiv:astro-ph/0509766](https://arxiv.org/abs/astro-ph/0509766) doi:10.1051/0004-6361:200500196.
- [9] E. Molinari, S. D. Vergani, D. Malesani, et al. REM observations of GRB 060418 and GRB 060607A: the onset of the afterglow and the initial fireball Lorentz factor determination. *A&A* **469**:L13–L16, 2007. [arXiv:astro-ph/0612607](https://arxiv.org/abs/astro-ph/0612607) doi:10.1051/0004-6361:20077388.
- [10] C. C. Thöne, D. A. Kann, G. Jóhannesson, et al. Photometry and spectroscopy of GRB 060526: a detailed study of the afterglow and host galaxy of a $z = 3.2$ gamma-ray burst. *A&A* **523**:A70, 2010. [arXiv:0806.1182](https://arxiv.org/abs/0806.1182) doi:10.1051/0004-6361/200810340.
- [11] P. Ferrero, S. Klose, D. A. Kann, et al. GRB 060605: multi-wavelength analysis of the first GRB observed using integral field spectroscopy. *A&A* **497**:729–741, 2009. [arXiv:0804.2457](https://arxiv.org/abs/0804.2457) doi:10.1051/0004-6361/200809980.

- [12] M. Nysewander, D. E. Reichart, J. A. Crain, et al. Prompt Observations of the Early-Time Optical Afterglow of GRB 060607A. *ApJ* **693**:1417–1423, 2009. [arXiv:0708.3444](#) DOI:10.1088/0004-637X/693/2/1417.
- [13] E. S. Rykoff, F. Aharonian, C. W. Akerlof, et al. Looking Into the Fireball: ROTSE-III and Swift Observations of Early Gamma-ray Burst Afterglows. *ApJ* **702**:489–505, 2009. [arXiv:0904.0261](#) DOI:10.1088/0004-637X/702/1/489.
- [14] A. Klotz, B. Gendre, G. Stratta, et al. Early emission of rising optical afterglows: the case of GRB 060904B and GRB 070420. *A&A* **483**:847–855, 2008. [arXiv:0803.0505](#) DOI:10.1051/0004-6361:20078677.
- [15] K. L. Page, R. Willingale, J. P. Osborne, et al. GRB 061121: Broadband Spectral Evolution through the Prompt and Afterglow Phases of a Bright Burst. *ApJ* **663**:1125–1138, 2007. [arXiv:0704.1609](#) DOI:10.1086/518821.
- [16] H. Mikuz, J. Skvarc, B. Dintinjana. GRB 070411: optical photometry at crni vrh. *GRB Coordinates Network* **6288**:1, 2007.
- [17] E. S. Rykoff, W. Rujopakarn, R. Quimby, et al. GRB 070411: ROTSE-III detection of optical counterpart. *GRB Coordinates Network* **6269**:1, 2007.
- [18] D. A. Kann, U. Laux, S. Klose, et al. GRB 070411: TLS data shows plateau, flares. *GRB Coordinates Network* **6295**:1, 2007.
- [19] A. Gomboc, A. Melandri, C. G. Mundell, et al. GRB 070411 : Liverpool telescope observations. *GRB Coordinates Network* **6271**:1, 2007.
- [20] M. Jelinek, J. A. Caballero, A. de La Nuez, A. J. Castro-Tirado. GRB 070411: IAC80 optical observations. *GRB Coordinates Network* **6272**:1, 2007.
- [21] P. Ferrero, S. Klose, D. A. Kann, S. Schulze. GRB 070411: deep VLT detection. *GRB Coordinates Network* **6319**:1, 2007.
- [22] D. A. Perley, J. S. Bloom, R. J. Foley, D. Kocevski. GRB 070411: late-time Keck imaging. *GRB Coordinates Network* **6350**:1, 2007.
- [23] A. Melandri, C. Guidorzi, S. Kobayashi, et al. Evidence for energy injection and a fine-tuned central engine at optical wavelengths in GRB 070419A. *MNRAS* **395**:1941–1949, 2009. [arXiv:0903.1414](#) DOI:10.1111/j.1365-2966.2009.14729.x.
- [24] S. Covino, P. D’Avanzo, A. Klotz, et al. The complex light curve of the afterglow of GRB071010A. *MNRAS* **388**:347–356, 2008. [arXiv:0804.4367](#) DOI:10.1111/j.1365-2966.2008.13393.x.
- [25] J. H. Wang, M. E. Schwamb, K. Y. Huang, et al. Early Optical Brightening in GRB 071010B. *ApJL* **679**:L5–L8, 2008. DOI:10.1086/588814.
- [26] D. A. Perley, J. S. Bloom, C. R. Klein, et al. Evidence for supernova-synthesized dust from the rising afterglow of GRB071025 at $z \sim 5$. *MNRAS* **406**:2473–2487, 2010. [arXiv:0912.2999](#) DOI:10.1111/j.1365-2966.2010.16772.x.
- [27] T. Krühler, J. Greiner, S. McBreen, et al. Correlated Optical and X-Ray Flares in the Afterglow of XRF 071031. *ApJ* **697**:758–768, 2009. [arXiv:0903.1184](#) DOI:10.1088/0004-637X/697/1/758.
- [28] J. Greiner, T. Krühler, S. McBreen, et al. A Strong Optical Flare Before the Rising Afterglow of GRB 080129. *ApJ* **693**:1912–1919, 2009. [arXiv:0811.4291](#) DOI:10.1088/0004-637X/693/2/1912.
- [29] F. E. Marshall, D. Grupe. GRB 080210: Swift/UVOT refined analysis. *GRB Coordinates Network* **7292**:1, 2008.
- [30] A. Klotz, M. Boer, J. L. Atteia. GRB 080210: TAROT la silla observatory optical detection. *GRB Coordinates Network* **7280**:1, 2008.
- [31] P. Jakobsson, P. M. Vreeswijk, D. Malesani, et al. GRB 080210: VLT redshift. *GRB Coordinates Network* **7286**:1, 2008.
- [32] A. C. Updike, G. G. Williams, P. A. Milne, et al. GRB 080210: Super-LOTIS observations. *GRB Coordinates Network* **7288**:1, 2008.
- [33] D. A. Perley, M. Modjaz, J. S. Bloom, et al. GRB 080210: Keck photometry. *GRB Coordinates Network* **7298**:1, 2008.
- [34] P. M. Vreeswijk, C. Ledoux, A. J. J. Raassen, et al. Time-dependent excitation and ionization modelling of absorption-line variability due to GRB 080310. *A&A* **549**:A22, 2013. [arXiv:1209.1506](#) DOI:10.1051/0004-6361/201219652.
- [35] J. L. Racusin, S. V. Karpov, M. Sokolowski, et al. Broadband observations of the naked-eye γ -ray burst GRB080319B. *Nature* **455**:183–188, 2008. [arXiv:0805.1557](#) DOI:10.1038/nature07270.
- [36] C. Guidorzi, S. Kobayashi, D. A. Perley, et al. A faint optical flash in dust-obscured GRB 080603A: implications for GRB prompt emission mechanisms. *MNRAS* **417**:2124–2143, 2011. [arXiv:1105.1591](#) DOI:10.1111/j.1365-2966.2011.19394.x.
- [37] T. Krühler, J. Greiner, P. Afonso, et al. The bright optical/NIR afterglow of the faint GRB 080710 - evidence of a jet viewed off-axis. *A&A* **508**:593–598, 2009. [arXiv:0908.2250](#) DOI:10.1051/0004-6361/200912649.
- [38] K. L. Page, R. Willingale, E. Bissaldi, et al. Multiwavelength observations of the energetic GRB 080810: detailed mapping of the broad-band spectral evolution. *MNRAS* **400**:134–146, 2009. [arXiv:0907.4578](#) DOI:10.1111/j.1365-2966.2009.15462.x.
- [39] A. Rossi, S. Schulze, S. Klose, et al. The Swift/Fermi GRB 080928 from 1 eV to 150 keV. *A&A* **529**:A142, 2011. [arXiv:1007.0383](#) DOI:10.1051/0004-6361/201015324.
- [40] Z.-P. Jin, S. Covino, M. Della Valle, et al. GRB 081007 and GRB 090424: The Surrounding Medium, Outflows, and Supernovae. *ApJ* **774**:114, 2013. [arXiv:1306.4585](#) DOI:10.1088/0004-637X/774/2/114.
- [41] F. Yuan, P. Schady, J. L. Racusin, et al. GRB 081008: From Burst to Afterglow and the Transition Phase in Between. *ApJ* **711**:870–880, 2010. [arXiv:1002.0581](#) DOI:10.1088/0004-637X/711/2/870.
- [42] N. P. M. Kuin, W. Landsman, M. J. Page, et al. GRB 081203A: Swift UVOT captures the earliest ultraviolet spectrum of a gamma-ray burst. *MNRAS* **395**:L21–L24, 2009. [arXiv:0812.2943](#) DOI:10.1111/j.1745-3933.2009.00632.x.

- [43] A. Melandri, S. Kobayashi, C. G. Mundell, et al. GRB 090313 and the Origin of Optical Peaks in Gamma-ray Burst Light Curves: Implications for Lorentz Factors and Radio Flares. *ApJ* **723**:1331–1342, 2010. [arXiv:1009.4361](https://arxiv.org/abs/1009.4361) DOI:10.1088/0004-637X/723/2/1331.
- [44] J. Wren, W. T. Vestrand, P. R. Wozniak, et al. GRB 090530: early RAPTOR optical observations. *GRB Coordinates Network* **9478**:1, 2009.
- [45] A. Rossi, F. Olivares, J. Greiner. GRB 090530: break in light curve. *GRB Coordinates Network* **9458**:1, 2009.
- [46] V. Šimon, C. Polášek, M. Jelínek, et al. Complicated variations in the early optical afterglow of GRB 090726. *A&A* **510**:A49, 2010. [arXiv:0911.1778](https://arxiv.org/abs/0911.1778) DOI:10.1051/0004-6361/200913393.
- [47] A. Updike, A. Rau, T. Kruehler, et al. GRB 090812: GROND observations of the Optical/NIR afterglow. *GRB Coordinates Network* **9773**:1, 2009.
- [48] J. Wren, W. T. Vestrand, P. R. Wozniak, et al. GRB 090812: RAPTOR detections during the burst. *GRB Coordinates Network* **9778**:1, 2009.
- [49] R. Filgas, J. Greiner, P. Schady, et al. GRB 091029: at the limit of the fireball scenario. *A&A* **546**:A101, 2012. [arXiv:1209.4658](https://arxiv.org/abs/1209.4658) DOI:10.1051/0004-6361/201219583.
- [50] E. S. Gorbovskoy, G. V. Lipunova, V. M. Lipunov, et al. Prompt, early and afterglow optical observations of five γ -ray bursts: GRB 100901A, GRB 100902A, GRB 100905A, GRB 100906A and GRB 101020A. *MNRAS* **421**:1874–1890, 2012. [arXiv:1111.3625](https://arxiv.org/abs/1111.3625) DOI:10.1111/j.1365-2966.2012.20195.x.
- [51] B. Gendre, J. L. Atteia, M. Boér, et al. GRB 110205A: Anatomy of a Long Gamma-Ray Burst. *ApJ* **748**:59, 2012. [arXiv:1110.0734](https://arxiv.org/abs/1110.0734) DOI:10.1088/0004-637X/748/1/59.
- [52] A. Cucchiara, S. B. Cenko, J. S. Bloom, et al. Constraining Gamma-Ray Burst Emission Physics with Extensive Early-time, Multiband Follow-up. *ApJ* **743**:154, 2011. [arXiv:1107.3352](https://arxiv.org/abs/1107.3352) DOI:10.1088/0004-637X/743/2/154.
- [53] N. R. Butler, D. Kocevski, J. S. Bloom, J. L. Curtis. A Complete Catalog of Swift Gamma-Ray Burst Spectra and Durations: Demise of a Physical Origin for Pre-Swift High-Energy Correlations. *ApJ* **671**:656–677, 2007. [arXiv:0706.1275](https://arxiv.org/abs/0706.1275) DOI:10.1086/522492.
- [54] A. Panaiteescu, W. T. Vestrand, P. Woźniak. Peaks of optical and X-ray afterglow light curves. *MNRAS* **433**:759–770, 2013. [arXiv:1305.0809](https://arxiv.org/abs/1305.0809) DOI:10.1093/mnras/stt769.
- [55] D. A. Kann, S. Klose, B. Zhang, et al. The Afterglows of Swift-era Gamma-ray Bursts. I. Comparing pre-Swift and Swift-era Long/Soft (Type II) GRB Optical Afterglows. *ApJ* **720**:1513–1558, 2010. [arXiv:0712.2186](https://arxiv.org/abs/0712.2186) DOI:10.1088/0004-637X/720/2/1513.
- [56] Y. C. Pei. Interstellar dust from the Milky Way to the Magellanic Clouds. *ApJ* **395**:130–139, 1992. DOI:10.1086/171637.
- [57] D. M. Coward, E. J. Howell, M. Branchesi, et al. The Swift gamma-ray burst redshift distribution: selection biases and optical brightness evolution at high z ? *MNRAS* **432**:2141–2149, 2013. [arXiv:1210.2488](https://arxiv.org/abs/1210.2488) DOI:10.1093/mnras/stt537.
- [58] L. J. Gou, P. Mészáros, T. Abel, B. Zhang. Detectability of Long Gamma-Ray Burst Afterglows from Very High Redshifts. *ApJ* **604**:508–520, 2004. [arXiv:astro-ph/0307489](https://arxiv.org/abs/astro-ph/0307489) DOI:10.1086/382061.
- [59] A. Panaiteescu. Gamma-Ray Burst afterglows: theory and observations. In C. Meegan, C. Kouveliotou, N. Gehrels (eds.), *American Institute of Physics Conference Series*, vol. 1133 of *American Institute of Physics Conference Series*, pp. 127–138. 2009. [arXiv:0812.1038](https://arxiv.org/abs/0812.1038) DOI:10.1063/1.3155864.
- [60] T. Piran. The physics of gamma-ray bursts. *Reviews of Modern Physics* **76**:1143–1210, 2004. [arXiv:astro-ph/0405503](https://arxiv.org/abs/astro-ph/0405503) DOI:10.1103/RevModPhys.76.1143.
- [61] T. Zafar, D. Watson, J. P. U. Fynbo, et al. The extinction curves of star-forming regions from $z = 0.1$ to 6.7 using GRB afterglow spectroscopy. *A&A* **532**:A143, 2011. [arXiv:1102.1469](https://arxiv.org/abs/1102.1469) DOI:10.1051/0004-6361/201116663.
- [62] A. Panaiteescu, W. T. Vestrand. Optical afterglows of gamma-ray bursts: peaks, plateaus and possibilities. *MNRAS* **414**:3537–3546, 2011. [arXiv:1009.3947](https://arxiv.org/abs/1009.3947) DOI:10.1111/j.1365-2966.2011.18653.x.
- [63] E.-W. Liang, S.-X. Yi, J. Zhang, et al. Constraining Gamma-ray Burst Initial Lorentz Factor with the Afterglow Onset Feature and Discovery of a Tight Γ_0 -E_{iso} Correlation. *ApJ* **725**:2209–2224, 2010. [arXiv:0912.4800](https://arxiv.org/abs/0912.4800) DOI:10.1088/0004-637X/725/2/2209.
- [64] J. Lü, Y.-C. Zou, W.-H. Lei, et al. Lorentz-factor-Isotropic-luminosity/Energy Correlations of Gamma-Ray Bursts and Their Interpretation. *ApJ* **751**:49, 2012. [arXiv:1109.3757](https://arxiv.org/abs/1109.3757) DOI:10.1088/0004-637X/751/1/49.
- [65] R. Sari, T. Piran. Predictions for the Very Early Afterglow and the Optical Flash. *ApJ* **520**:641–649, 1999. [arXiv:astro-ph/9901338](https://arxiv.org/abs/astro-ph/9901338) DOI:10.1086/307508.
- [66] P. Mészáros. Gamma-ray bursts. *Reports on Progress in Physics* **69**:2259–2321, 2006. [arXiv:astro-ph/0605208](https://arxiv.org/abs/astro-ph/0605208) DOI:10.1088/0034-4885/69/8/R01.
- [67] J. Schaye, C. Dalla Vecchia. On the relation between the Schmidt and Kennicutt-Schmidt star formation laws and its implications for numerical simulations. *MNRAS* **383**:1210–1222, 2008. [arXiv:0709.0292](https://arxiv.org/abs/0709.0292) DOI:10.1111/j.1365-2966.2007.12639.x.
- [68] List of GRB hosts. [2014-08-06], <http://grbhosts.org>.
- [69] B. Ciardi, A. Loeb. Expected Number and Flux Distribution of Gamma-Ray Burst Afterglows with High Redshifts. *ApJ* **540**:687–696, 2000. [arXiv:astro-ph/0002412](https://arxiv.org/abs/astro-ph/0002412) DOI:10.1086/309384.
- [70] G. Rodighiero, G. L. Granato, A. Franceschini, et al. Spiral and irregular galaxies in the Hubble Deep Field North. Comparison with early types and implications for the global SFR density. *A&A* **364**:517–531, 2000. [arXiv:astro-ph/0010131](https://arxiv.org/abs/astro-ph/0010131).
- [71] J. Mao. A Theoretical Investigation of Gamma-ray Burst Host Galaxies. *ApJ* **717**:140–146, 2010. [arXiv:1005.1876](https://arxiv.org/abs/1005.1876) DOI:10.1088/0004-637X/717/1/140.